C 55.13: NESS 70

NOAA Technical Report NESS 70

Compatibility of Low-Cloud Vectors and Rawins for Synoptic Scale Analysis

DEPARTMENT OF COMMERCE
UNITED STATES OF AMERICA

WASHINGTON, D.C.
OCTOBER 1974

TATE UNIVERSITY
COLLECTION

noaa NATIONAL OCEANIC AND ATMOSPHERIC ADMINISTRATION / National Environmental Satellite Service

NOAA TECHNICAL REPORTS

National Environmental Satellite Service Series

The National Environmental Satellite Service (NESS) is responsible for the establishment and operation of the environmental satellite systems of NOAA.

Publication of a report in NOAA Technical Report NESS series will not preclude later publication in an expanded or modified form in scientific journals. NESS series of NOAA Technical Reports is a continuation of, and retains the consecutive numbering sequence of, the former series, ESSA Technical Report National Environmental Satellite Center (NESC), and of the earlier series, Weather Bureau Meteorological Satellite Laboratory (MSL) Report. Reports 1 through 37 are listed in publication NESC 56 of this series.

Reports 1 through 50 in the series are available from the National Technical Information Service (NTIS), U.S. Department of Commerce, Sills Bldg., 5285 Port Royal Road, Springfield, Va. 22151, in paper copy or microfiche form. Order by accession number, when given, in parentheses. Beginning with 51, printed copies of the reports are available through the Superintendent of Documents, U.S. Government Printing Office, Washington, D.C. 20402; microfiche available from NTIS (use accession number when available). Prices given on request from the Superintendent of Documents or NTIS.

ESSA Technical Reports

NESC 38 Angular Distribution of Solar Radiation Reflected From Clouds as Determined From TIROS IV Radiometer Measurements. I. Ruff, R. Koffler, S. Fritz, J. S. Winston, and P. K. Rao, March 1967. (PB-174-729)

NESC 39 Motions in the Upper Troposphere as Revealed by Satellite Observed Cirrus Formations. H. McClure Johnson, October 1966. (PB-173-996)

NESC 40 Cloud Measurements Using Aircraft Time-Lapse Photography. Linwood F. Whitney, Jr., and E. Paul McClain, April 1967. (PB-174-728)

NESC 41 The SINAP Problem: Present Status and Future Prospects; Proceedings of a Conference Held at the National Environmental Satellite Center, Suitland, Maryland, January 18-20, 1967. E. Paul McClain, October 1967. (PB-176-570)

NESC 42 Operational Processing of Low Resolution Infrared (LRIR) Data From ESSA Satellites. Louis Rubin, February 1968. (PB-178-123)

NESC 43 Atlas of World Maps of Long-Wave Radiation and Albedo--for Seasons and Months Based on Measurements From TIROS IV and TIROS VII. J. S. Winston and V. Ray Taylor, September 1967. (PB-176-569)

NESC 44 Processing and Display Experiments Using Digitized ATS-1 Spin Scan Camera Data. M. B. Whitney, R. C. Doolittle, and B. Goddard, April 1968. (PB-178-424)

NESC 45 The Nature of Intermediate-Scale Cloud Spirals. Linwood F. Whitney, Jr., and Leroy D. Herman, May 1968. (AD-673-681)

NESC 46 Monthly and Seasonal Mean Global Charts of Brightness From ESSA 3 and ESSA 5 Digitized Pictures, February 1967-February 1968. V. Ray Taylor and Jay S. Winston, November 1968. (PB-180-717)

NESC 47 A Polynomial Representation of Carbon Dioxide and Water Vapor Transmission. William L. Smith, February 1969. (PB-183-296)

NESC 48 Statistical Estimation of the Atmosphere's Geopotential Height Distribution From Satellite Radiation Measurements. William L. Smith, February 1969. (PB-183-297)

NESC 49 Synoptic/Dynamic Diagnosis of a Developing Low-Level Cyclone and Its Satellite-Viewed Cloud Patterns. Harold J. Brodrick and E. Paul McClain, May 1969. (PB-184-612)

NESC 50 Estimating Maximum Wind Speed of Tropical Storms From High Resolution Infrared Data. L. F. Hubert, A. Timchalk, and S. Fritz, May 1969. (PB-184-611)

(Continued on inside back cover)

NOAA Technical Report NESS 70

Compatibility of Low-Cloud Vectors and Rawins for Synoptic Scale Analysis

L. F. HUBERT AND L. F. WHITNEY, JR.

WASHINGTON, D.C.
OCTOBER 1974

U. S. Depository Copy

UNITED STATES
DEPARTMENT OF COMMERCE
Frederick B. Dent, Secretary

NATIONAL OCEANIC AND
ATMOSPHERIC ADMINISTRATION
Robert M. White, Administrator

National Environmental
Satellite Service
David S. Johnson, Director

CONTENTS

Abstract............................ 1
I. Introduction.................. 2
II. Data and analysis method....... 3
A. Data..................... 3
B. Analysis................. 4
III. Experiment 1.................. 5
IV. Experiment 2.................. 8
A. Data and procedure........ 9
B. Results and interpretation 10
V. Conclusions................... 12
Acknowledgments.................... 13
References......................... 13
Figures and tables................. 14

Mention of a commercial company or product does not constitute an endorsement by the NOAA National Environmental Satellite Service. Use for publicity or advertising purposes of information from this publication concerning proprietary products or the tests of such products is not authorized.

For sale by the Superintendent of Documents, Government
Printing Office Washington, D.C., 20402 - Price 75 cents

COMPATIBILITY OF LOW-CLOUD VECTORS AND RAWINS FOR SYNOPTIC SCALE ANALYSIS

L. F. Hubert and L. F. Whitney, Jr.
Meteorological Satellite Laboratory,
National Environmental Satellite Service, NOAA, Washington, D.C.

ABSTRACT. Low-cloud motions derived by both manual and computer techniques from geosynchronous satellite data and rawin observations are analyzed in various combinations for a two-part analysis compatibility experiment. Since the true air motion is unknown, compatibility rather than absolute accuracy of these three data sets is examined.

The intent of experiment 1 is to establish a series of "best" analyses of the low troposphere over a large Pacific Ocean region for a 5-day period in August 1972 and to determine the compatibility of the various data sets with that series of best analyses. The most meaningfully detailed and time-continuous analyses resulted from a daily combination of all data sets. Despite large variations in the amount of data among the sets, each deviated from the analyses by about the same magnitude (viz, a mean of about 3 kt).

Experiment 2 concerns reanalysis of a subarea (of the experiment 1 analysis) containing most of the rawin stations. The purpose of experiment 2 is to examine the compatibility of independent analyses of each data set after removing differences in sample number and distribution and while maintaining the same boundary conditions. Analyses of rawin, computer, and manual vectors differ by a 6-kt mean vector magnitude but appear to yield the same synoptic scale analyses to within a mean vector difference of 3 kt.

Two other important points are brought out by this study:
(1) Increased density and better distribution of wind data provided by geosynchronous satellites control analyses so that severe editing is unnecessary (i.e., good data distribution and density overcome the effect of a few bad data), and (2) the analyses illustrate a shortcoming of these satellite wind data. Since low-cloud vectors are obtained only at the periphery and not within disturbances, the intensity of disturbances is underestimated. Availability of infrared data from geosynchronous satellites will increase the number of middle- or high-cloud vectors in or near these disturbances. These additional vectors may aid in better depicting the intensity of disturbances.

I. INTRODUCTION

For several years, the National Environmental Satellite Service routinely has been measuring cloud vectors (Fujita et al. 1968, Young et al. 1972) from animated sequences of pictures taken from geosynchronous satellites (ATS 1 and ATS 3, the Applications Technology Satellites). More recently, low level cloud vectors also have been derived operationally by a computer technique (Leese et al. 1971) using cross correlation of small arrays of brightness values from pairs of ATS pictures. Since many clouds are carried passively by the ambient air motion, both types of cloud vectors are utilized as wind estimates by various users such as the National Meteorological Center (NMC).

Our purpose in this investigation is to examine accuracy of these satellite data by means of synoptic scale analyses. In fact, accuracy cannot be assessed because we do not know the true field of motion--no absolute ground truth is available. Rather, we construct an analysis from a combination of data that subjectively is judged to be the best approximation to the real field of motion. Rawin observations and both types of cloud vectors then are compared to this best analysis. [We distinguish between cloud vectors obtained from animated sequences (manual vectors) and those obtained by the cross-correlation technique (computer vectors)].

These analysis experiments reveal the degree of compatibility of rawin and satellite data rather than their absolute accuracy. Nevertheless, a measure of accuracy is implied by compatibility for the following reason. All wind data contain errors and small-scale perturbations; therefore, smoothing with an analysis procedure is required to produce fields most representative of synoptic scale flow. Thus, deviations between individual observations and analyses are more appropriate measures of accuracy than are deviations between individual rawins and individual cloud vectors (considering that the chief use of cloud vectors is to derive synoptic scale analyses).

Earlier studies showed rather large differences between individual rawins and cloud vectors (Hubert and Whitney 1971). Clearly, it is improper to regard such differences as error due to only satellite data because those differences also include rawin errors, time and space changes of wind, and disparity of scales. The present work demonstrates that, for synoptic scale flow, rawins and low-cloud vectors probably are about equally representative. Our results are credible because rawins deviate from these best analyses no more than expected from independent studies of balloon observations (Hubert and Timchalk 1972, Lenhard 1973).

This study is restricted to low-level analyses because only low-level vectors are derived by the computer technique. Because low level cloud vectors correspond quite closely to 3,000-ft to 5,000-ft balloon winds (Hubert and Whitney 1971), only the 850-mb and 5,000-ft rawin data were assembled for these low-level analyses.[1] Two independent experiments with the same data base and objective analysis procedure are reported here.

Our goal in experiment 1 was to derive a "best" analysis of the 850-mb or 5,000-ft wind field and to determine how well the analyses fit the observations. Various combinations of data were examined, and a 5-day sequence of best analyses was produced for a large region of the Pacific Ocean. In experiment 2, we examined compatibility under more controlled conditions. A small portion of the larger area was reanalyzed with selected data. For the latter, satellite vectors were deleted selectively so that the number and distribution of each type of data (rawins, manual vectors, or computer vectors) were equivalent. Independent analyses of each type of data then were made to determine to what degree these different observations produced identical analyses. The similarities and differences support results of experiment 1 (viz, that 850-mb or 5,000-ft rawins and cloud vectors are about equally representative of synoptic scale flow). Characteristics of satellite data that affect their utilization are illustrated by this study.

II. DATA AND ANALYSIS METHOD

A. Data

Five days of Pacific observations for Aug. 13-17, 1972, supplied the data base for these experiments. Choice of time and area was determined by our requirement for a large number of rawin observations simultaneous with a good distribution of manual and computer vectors. The area chosen lay between 36°N and 36°S and 110°W westward to 160°E. An archive of all manual and computer vectors together with 00 GMT rawins for 850 mb or 5,000 ft was used in this study.

Computer vectors had been derived operationally from arrays centered at 5° latitude-longitude intersections. Also in experiment 2, supplementary nonoperational computer vectors were centered at locations of the manual vectors, which were scattered throughout the area at irregular locations. Typically, 100 manual vectors and 200 to 250 computer vectors had been derived each day. Some 40 rawin stations supplied 22 to 28 wind observations per day.

The operationally derived computer vectors were edited successively first by automatic and then by subjective methods. For example, low-level winds greater than 40 kt were deleted. The archive, however, retained all deleted vectors with symbols indicating the reason for their deletion; therefore, all cloud vectors initially derived were available for our analysis and editing experiments. Figures 1C through 5C (grouped near the back of this study) show the data distribution of both rawins and cloud vectors, and figures 1A through 5A present one picture from each of the sequences that yielded cloud vectors. Synoptically, two tropical storms dominated the Northern Hemisphere circulation in this region, two frontal systems with a large anticyclone characterized the Southern Hemisphere circulation, and the intertropical convergence zone developed during the 5-day series.

---

[1] Some time after we had assembled our data set of 850-mb and 5,000-ft winds, some evidence was developed by different workers that low-cloud vectors may correspond slightly better to balloon winds at 2,000 ft (e.g., Hubert and Timchalk 1972, Poteat 1973). It was not feasible to reassemble our data and repeat the experiments with 2,000-ft winds.

B. Analysis

An objective scheme designed and programmed ty Thomasell (1973) produced all analyses for both parts of this investigation. It is a direct independent analysis of the u and v components that:

1. Exercises various edit options to delete data before analysis.

2. Produces a preliminary analysis from the selected set of data and a first guess.

3. Deletes data that differ from the preliminary analysis by a specified vector difference.[2]

4. Produces a final analysis using the surviving data and the preliminary analysis as the first guess.

5. Interpolates the final analysis to the location of the data and computes the magnitudes of vector deviations between final analysis and data (which are summarized as means $\overline{|\Delta \mathbf{V}|}$), root mean squares (rms), and standard deviations (σ).

6. Uses the final analysis as the first guess for the next day's analysis.

Boundary values for the analyses were taken from the operational NMC analysis of Aug. 13, 1972, and were held fixed for the 5-day sequence at grid points that extended two grid intervals outside our basic analysis area (36°N to 36°S and 110°W to 160°E). Boundary values of our basic analysis area changed from day to day, being determined by the first guess for that day's analysis. No deviation statistics were computed at or outside the boundary of the basic analysis area. Grid-point intervals were 2° latitude-longitude throughout both experiments.

Gradients of the first-guess fields were used to interpolate observations to their nearest grid point. Further influence of the first guess on the final analysis depends upon which of two options is chosen. Analyzed values at grid points that are not directly determined by observations or boundary values are interpolated with a relaxation routine. Poisson's equation is solved for nondata grid points with either

---

[2] The effects of different thresholds are discussed in topic III.

forcing function = Laplacian of the first guess (1)

or

forcing function = zero. (2)

The first option retains strong influence of the first guess at nondata grid points. The second linearly interpolates between data or boundary grid points (Thomasell and Welsh 1963).

The second option was used for this experiment because the previous day's analysis, used as the first guess, often degraded the analysis. For example, a moving trough might be delineated well by data on 2 days. If on the second day the region around the previous day's trough position had no new data, the first guess trough would be retained. The final analysis then would contain two troughs, one of which could be spurious.

Once the final analysis was obtained, vorticity and divergence were computed over two-grid intervals. Figures 1B through 5B are the analyses reproduced by a display technique programmed by Nagle (1973). Figures 1C through 5C show vorticity analyses superimposed on the wind data on which the analyses are based.

III. EXPERIMENT 1

The purpose of experiment 1 is to derive the best analysis of the low troposphere near 850 mb at about 00 GMT each day for Aug. 13-17, 1972, and to gain insight into characteristics of the analysis problems.

Having no absolute ground truth, the best analysis sequence was chosen subjectively, chiefly on grounds of reasonable synoptic scale patterns and good time continuity. Experience in correlating cloud photographs (figs. 1A through 5A) with synoptic features was useful in selecting the best analysis.

Many combinations of data and analysis options were used in this study. They are too voluminous to detail here, but the results can be summarized as:

1. The most meaningfully detailed and time-continuous analyses resulted from a combination of all three types of data.

This result was evident in streamline and vorticity patterns. Single types of data and combinations of only two types of data (e.g., rawins and computer vectors) failed to yield equally good pattern and continuity.

Superior analysis from all data types combined (figs. 1B through 5B) is due in large part to the superior distribution of the total data set. Each type, at one place or another in the 5-day sequence, failed to observe some synoptic feature, so the resulting analysis suffered.

2. Each type of data deviated by approximately the same average amount from the best analysis.

Table 1 (adjacent to fig. 6 near the end of the study) lists the measured rms deviations of vector magnitude between data and final analysis for each of the 5 days. Figure 6 summarizes those deviations for the entire period. In addition, a cumulative frequency curve from an earlier study (Hubert and Whitney 1971) is shown. These larger deviations are differences between individual 850-mb rawins and individual low-cloud vectors. The three left-hand curves represent the fit of three sets of data to a sequence of best analyses.

If the best analyses are accurate representations of the actual synoptic scale field of motion, the three curves show that rawin and cloud vectors contain about the same amount of nonrepresentative noise. For example, 50% of all types of observations deviate a maximum of 2- to 3-kt vector magnitude from the synoptic scale flow. In contrast, the right-hand curve shows much larger deviations between individual 850-mb rawins and individual cloud vectors; at the 50% cumulative frequency, the individual differences exceed 8-kt vector magnitude.

While the left-hand curves of figure 6 are within 1 kt of one another up through 70% cumulative frequency, table 1 shows appreciably greater rms differences between corresponding data. This disparity is due to a few rawins that fit the analysis quite poorly.

Notwithstanding the disparity of rms values, data compatibility is suggested by the similarities of the curves in figure 6 up through 70% cumulative frequency. As we shall see, this indication of compatibility is borne out in topic IV.

3. Editing is necessary.

Unrealistic patterns were introduced when analyses were made with unedited cloud vectors. Analyses contained noisy detail that had no time continuity. Some but not all of the various editing options improved the analyses.

We found it necessary to delete excessively large vectors--a straightforward step in this experiment where only low levels were involved. For the Tropics and subtropics considered here, an upper limit of 50 kt was found adequate to eliminate questionable vectors and yet allow for high speeds near disturbances.

At the time these computer vectors were derived operationally, an objective climatological procedure deleted all tropical vectors with a westerly component. This procedure has since been dropped, but it was an option examined in our study. Better definition of synoptic systems was obtained by ignoring this type of editing that was introduced originally to eliminate upper level cloud vectors. Since this constraint also eliminated valid low-level vectors near disturbances, the gain of deleting upper vectors was more than offset by the loss of information near disturbances.

Manual editing, the principal quality control of operational cloud vectors, was quite beneficial to these analyses. This step consists of deleting vectors that appear to be questionable on grounds of inconsistency with their neighbors or with the synoptic situation or because of the presence of upper or multilevel clouds. Consequently, computer vectors that had been derived from high clouds and would have degraded the analyses were eliminated by manual editing.

The effect on analyses of deleting data that deviated significantly from the preliminary analysis was examined. Three reanalyses of the series (not shown herein) were made using only data that deviated respectively by less than 15 kt, by less than 10 kt, and by less than 5 kt from the preliminary analysis. At each step, the analyses became smoother; and deviations between analyses and surviving data, of course, decreased. Significant details of smaller synoptic features were lost while the gross synoptic patterns were retained. No significant improvement such as time continuity, however, could be attributed to this objective type of difference editing, so the best analyses (figs. 1B through 5B) incorporated no such editing. We cannot conclude, however, that difference editing is always unnecessary. Another data set might contain a greater number of spurious vectors and therefore might benefit from difference editing. In this set, only 23 vectors out of some 1,000 deviated from the preliminary analysis by more than 15 kt.

In summary, the best data set for our experiments resulted from step (1) deletion of low-level vectors 50 kt or greater and step (2) inspection of computer vectors to screen out those that are inconsistent with the synoptic situation depicted by the cloud pattern or with nearby vectors.

Study of the various editing options yielded a rather surprising sidelight (viz, that the rms deviations between analyses or between data and analyses are, by themselves, not a sensitive measure of analysis quality. We found that the rms deviations listed in table 1 were about the same as those obtained from analysis of unedited vectors. Analysis quality must be judged not only on deviation statistics but also on the basis of time continuity and consistency with cloud patterns.

4. Intensities of many systems were poorly depicted.

The pattern of vorticity corresponds well with the synoptic systems,[3] but magnitudes (especially cyclonic vorticity) are poorly depicted. This shortcoming is exacerbated by limiting the analysis to a single low level. Middle and upper clouds obscure the low clouds in disturbances. As a result, cloud vectors are derived only on the periphery of disturbances. Such observations interpolated across the active portion of disturbances severely underestimate intensity. See, for example, the location of data and analysis of tropical storms in figures 1 through 5. Maximum vorticity does not exceed $5 \times 10^{-5}\ s^{-1}$ and depends more on the chance location of data than on the actual storm vorticity.

---

[3] On the other hand, divergence patterns (not shown) were poorly associated with the primary synoptic features.

Computer vectors are subject to this shortcoming to a greater degree than manual vectors, but it is characteristic of both types.

This characteristic is an important limitation of cloud vectors that largely has been neglected. The results here indicate that the number of cloud vectors can be a poor measure of meteorological information. It is easy to double or triple the number of low-cloud vectors; but sampling is likely to be increased only in undisturbed areas, while information in disturbed regions remains inadequate.

Availability of infrared observations from geosynchronous satellites may improve this situation. While the number of low-cloud vectors may not be increased, the number of middle- and high-cloud vectors in or near disturbances will be. These upper level vectors when supplied to an analysis procedure that enforces vertical consistency then might better depict the intensity of disturbances.

5. Residuals from questionable first-guess fields must be avoided.

As already mentioned, data distributed irregularly in time and space must be analyzed under a minimum influence of a mediocre first guess. While cloud vectors are more numerous and better distributed than conventional wind data, their distribution can suffer in localities of disturbances, for example. Therefore, an analysis of these vectors under the strong influence of a poor first guess can introduce spurious features.

IV. EXPERIMENT 2

The results of experiment 1 indicate that low-cloud vectors and 850-mb rawins complement each other and produce better analyses than would result from analysis of only one type of data. Cloud vectors are numerous and well distributed; therefore, the possibility exists than better analyses were the consequence of superior coverage of combined date although the different types of data represented somewhat different fields of motion. In experiment 2, we ask, "Do low-cloud vectors and 850-mb or 5,000-ft rawins represent the same synoptic scale field of motion?"

By their nature, balloons and cloud targets respond to very different scales of motion. To minimize differences between data types caused by small-scale perturbation, we analyzed the observations on a synoptic scale grid. Our experience with experiment 1 showed that analyses were sensitive to data distribution and boundary conditions. Steps 1 and 2 of the procedure listed below were followed to minimize the effect of variable data distribution and boundary values.

A. Data and Procedure

Analyses for experiment 2 involved only a fraction of the area used in experiment 1. The subarea (fig. 7) contains most of the rawin stations. Analyses of the smaller area proceeded as follows:

1. Boundary values for the subarea analyses were taken from each day's final analyses of the larger area (figs. 1B through 5B). Inside the subarea, the final analyses served as first guesses.

2. Manual vectors and computer vectors were deleted selectively so that the number and distribution of each type of vector was equivalent to the number and distribution of rawin observations for that day. Because manual vectors were not available in the southern part of the subarea on Aug. 13, 1972, it was impossible to select a set comparable to the other types of data on that day. Experiment 2 analyses, therefore, were reduced to a 4-day series--Aug. 14-17, 1972. The result was three sets of data on each of the 4 days, each set containing 17 to 20 observations per day.

3. The subarea was reanalyzed successively with 850-mb or 5,000-ft rawins, with computer vectors, and with manual vectors (examples in fig. 8) using the procedure described in experiment 1.

4. Analyzed fields were interpolated to the locations of the data in each case, and magnitudes of vector deviations were computed between analysis and observation. These vector deviations were summarized in terms of means ($\overline{|\Delta \mathbf{V}|}$), root mean squares (rms), and standard deviations (σ) of vector magnitude (table 2).

5. Vorticity (fig. 8) and divergence fields were computed and compared.

6. Analyzed fields were compared at grid points *in the immediate vicinity of data* (table 3 and fig. 9).

B. Results and Interpretation

Tables 2 and 3 and figure 9 pertain to relatively few specific locations in the subarea (fig. 7) The locations were chosen to eliminate the influence of variable data amounts and distribution. Table 2 pertains to 17 to 20 wind observations per day per data type--a total of 72 per data type for the 4-day series. Table 3 and figure 9 pertain to 20 grid points per day per data type--a total of 80 per data type for the series.

Table 2 lists the degree of fit between individual observations and analyzed fields of motion. Along the table diagonal (bracketed items) are deviations between data and the analyses produced from those same data. These numerical values, therefore, represent the amount of smoothing introduced by the analysis procedure and provide the baseline for interpreting all other deviations.

Deviations such as those in table 3 must be interpreted in terms of such a baseline for the following reason: small-scale perturbations (i.e., the nonrepresentative components of observations) are suppressed by analysis procedures, but the degree of smoothing also is determined partly by the length of the grid interval and the procedure used to fit analyses to the data. (A different analysis procedure and different grid intervals could produce a different baseline.) Deviations between observations and the analyses made from those observations may, therefore, be regarded as the lower limit of deviations that can be expected between analyses such as those compared in table 3. Table 2 shows a range of rms (along the diagonal) of 3.0 to 3.9 kt; therefore, we might expect rms deviations of this magnitude in table 3, even if all types of data were completely compatible and contained exactly the same amount of random noise.

To compare the nonbracketed entries of table 2 with corresponding items from the bottom line of table 1 is instructive. The latter are deviations between individual observations and the best analyses for the entire area of experiment 1 but only for the 4-day series of experiment 2. Each type of data fits the combined-data analyses more closely than it fits analyses made with any single type of data. This again illustrates the benefit of combining all data. Figure 8 illustrates the reason for large deviations appearing in table 2.

Figure 8A is the streamline analysis of 850 mb rawin-only observations for August 14, and figure 8B is the analysis of manual cloud-vectors-only for the same day. While the synoptic scale trough and ridge patterns are very similar, the details are quite different. Cloud vectors depict an open trough and ridge while analysis of the rawins shows a closed cyclone and anticyclone. Large vector differences appear near singularity points. To compare figure 8 with figure 2B is also interesting. Vector-magnitude deviations (not shown) between the best analysis and these limited-data analyses show that both of the latter are more similar to the best analysis than they are to each other.

Isolines of relative vorticity also may be compared in figure 8. Consistent with the streamline analyses, large-scale features are similar. Vorticity magnitudes are small; no significant differences are apparent. The total vorticity range for rawin analysis is 2.0 to -1.5 x 10^{-5} s^{-1} while the range of cloud-vector analyses is 0.8 to -1.3 x 10^{-5} s^{-1}. In such flat fields, the differences in locations--by a grid point or so--of maxima and minima are to be expected.

Table 3 and figure 9 address the question asked earlier (viz, "Do cloud vectors and 850-mb rawins represent the same synoptic scale field of motion?"

The bottom line of table 3 shows average vector deviations between rawin analyses and cloud-vector analyses to be 6 kt. Notice that this is a factor 1.5 to 2 times greater than the baseline discussed in connection with table 2. A deviation considerably greater than the baseline indicates that cloud vectors and 850-mb rawins produce somewhat different synoptic scale analyses.

If rawin-only analyses were assumed to be perfectly accurate, the cloud-vector analyses would be inaccurate by a 6-kt mean vector magnitude. If, on the other hand the cloud-vector-only analyses were assumed to be perfectly accurate, the rawin-only analysis would be inaccurate by 6 kt. Neither assumption is acceptable. Experiment 2 suggests that analyses of a single type of data are inferior to the analyses of combined data. Consequently, we must conclude that the actual field of motion lies somewhere between the two single-data-type analyses and that the 6-kt error is divided between them. As a first approximation, we might assume each analysis to be in error by about a 3-kt mean vector error. We can regard 850-mb rawins and cloud vectors to be compatible to that same degree (i.e., they represent the actual synoptic scale flow field to about the same degree0 with errors of about 3-kt mean vector magnitude. One should note that these statistics and these conclusions pertain to low-level flow that is only weakly perturbed. We cannot apply these results to other levels or to highly disturbed low levels.

Evidence that cloud vectors and 850-mb rawins yield slightly different synoptic scale analyses also can be discerned by comparing deviations between computer and manual vectors with deviations between cloud vectors and rawins. The last set of columns (table 3, manual-computer) show smaller deviations than either of the first two sets of columns (manual-rawin and computer-rawin), with the exception of August 15, which is discussed later. These comparisons indicate that manual and computer cloud vectors are more compatible with each other (deviations approaching the baseline) than they are with the 850-mb rawins.

Finally, we see from table 3 that manual and computer vectors do not yield identical analyses, even excepting the August 15. At first glance, this is surprising because both types of vectors were derived from essentially the same cloud targets. Two factors are responsible for most of the data differences: (1) Granularity of computer vectors, especially for low speeds and (2) different registration errors in picture pairs and in movie loops.

Granularity is caused by computer vectors being derived only to the nearest integral picture element. Consider an extreme case where the cloud array moves only one picture element in the 0.5-hr interval between pictures (viz, 3 n.mi.). The derived direction, therefore, could be only one of four compass points and the speed resolved to no better than 6 kt. Manual vectors, on the other hand, are derived from cloud trajectories over periods of 2 to 2.5 hr , so granularity is proportionally reduced. Deviations between manual and computer vectors attributable to this factor are probably random so that over a large number of cases the mean deviation approaches zero.

Registration differences introduce different errors (different apparent landmark motion). Such differences are systematic for any one analysis period but may be random over a series of days--an effect apparent in the last two columns of table 3. Algebraic means of the meridional wind deviations ($\overline{\Delta v}$) and zonal wind deviations ($\overline{\Delta u}$) are very small for the 4-day series (at least 0.5 kt can be accounted for by granularity alone); but on August 15, the 6.9-kt difference in $\overline{\Delta u}$ strongly suggests registration differences in the east-west direction.

While both registration procedures may have contributed to this difference, visual landmark matching used for movie loop registration is suspect. Low contrast landmarks and the pressure of operational deadlines creates opportunity for human error. Other entries for August 15 in table 3 support our suspicion of movie loop registration. Notice that the mean vector magnitude and the zonal component ($\overline{\Delta u}$) for manual-rawin deviations is larger on August 15 than on any other day.

V. CONCLUSIONS

Experiment 1 demonstrated that the "best" synoptic scale analyses were obtained by combining 850-mb rawins, computer cloud vectors, and manual cloud vectors. Such a result is encouraging, for it suggests that these satellite data require no special weighting when combined with other types of wind observation for synoptic analysis. It appears that 70% of the various types of data all fit the best analysis to about the same degree, within a vector magnitude of 3 kt.

This experiment illustrates the need and value of editing, but it also shows that good data density overcomes a few erroneous data so that editing need not be severe. On balance, it appears best to admit a few questionable vectors if, but only if, data density and distribution are good. Over oceans, such density can be achieved only by use of cloud vectors.

An important shortcoming of cloud vectors is that intensities of disturbances are poorly depicted. While this may be ameliorated to some extent by using clouds at all levels (in contrast to the single levels used here), it may continue as a problem. This problem is persistent because dense uniform cloud cover characterizes many disturbances so that good cloud tracers frequently cannot be discerned within disturbances. Restricting analyses to a single low level exacerbates this fault because low-level clouds are obscured near disturbances. Only weakly perturbed flow on the outskirts of disturbances could be interpolated into the highly disturbed region.

Infrared data from geosynchronous satellites will enable us to determine more middle- and high-cloud vectors in and near disturbances. While low-level vectors will still be missing, incorporating higher level cloud vectors into a three-dimensional analysis may improve the description of disturbances.

Finally, experiment 2 indicates that low-cloud vectors are compatible with 850-mb rawins for analyzing synoptic scale flow. Both data sets may introduce about a 3-kt mean vector error. Other studies suggest that 2,000-ft rawins may correspond somewhat closer to low-cloud vectors, but our data did not enable us to examine this question. The possibility exists that the 3-kt error might be slightly reduced had 2,000-ft rawins been analyzed.

ACKNOWLEDGMENTS

In particular, we thank Albert Thomasell of the Meteorological Satellite Laboratory not only for the extensive programming effort involved in this study but also for his helpful suggestions in the interpretation of results.

Fred Nagle, also of our laboratory, contributed and helped adapt his objective streamline and isotach analysis scheme to Thomasell's analysis program.

REFERENCES

Fujita, Tetsuya, Bradbury, Dorothy L., Murino, Clifford, and Hull, Louis, "A Study of Mesoscale Cloud Motions Computed From ATS-1 and Terrestrial Photographs," Satellite and Mesometeorology Research Project Research Paper No. 71, ESSA Grant CWB WGB-34 and NSF Grants GA-864 and GA-410, Department of Geophysical Sciences, University of Chicago, Ill., Mar. 1968, 25 pp.

Hubert, Lester F., and Timchalk, Andrew, "Convective Clouds as Tracers of Air Motion," NOAA Technical Memorandum NESS 40, National Environmental Satellite Service, National Oceanic and Atmospheric Administration, U.S. Department of Commerce, Washington, D.C., Aug. 1972, 12 pp.

Hubert, Lester F., and Whitney, Linwood F., Jr., "Wind Estimation From Geostationary-Satellite Pictures," Monthly Weather Review, Vol. 99, No. 9, Sept. 1971, pp. 665-672.

Leese, John A., Novak, Charles S., and Clark, Bruce B., "An Automated Technique for Obtaining Cloud Motion From Geosynchronous Satellite Data Using Cross Correlation," Journal of Applied Meteorology, Vol. 10, No. 1, Feb. 1971, pp. 118-132.

Lenhard, Robert W., "Variability of Wind Over a Distance of 16.25 km," Journal of Applied Meteorology, Vol. 12, No. 6, Sept. 1973, pp. 1075-1078.

Nagle, Fred (Meteorological Satellite Laboratory, National Environmental Satellite Service, National Oceanic and Atmospheric Administration, U.S. Department of Commerce, Washington, D.C.), 1973 (personal communication).

Poteat, Kenneth O., "A Comparison of Satellite-Derived Low-Level and Cirrus-Level Winds With Conventional Wind Observations," Journal of Applied Meteorology, Vol. 12, No. 8, Dec. 1973, pp. 1416-1419.

Thomasell, Albert, Jr. (Meteorological Satellite Laboratory, National Environmental Satellite Service, National Oceanic and Atmospheric Administration, U.S. Department of Commerce, Washington, D.C.), 1973 (personal communication).

Thomasell, Albert, Jr., and Welsh, James G., "Studies of Techniques for the Analysis and Prediction of Temperature in the Ocean, Part 1: The Objective Analysis of Sea-Surface Temperature," Interim Report, U.S. Naval Oceanographic Office Contract N62306-905, The Travelers Research Center, Inc., Hartford, Conn., July 1963, 52 pp.

Young, Michael T., Doolittle, Russell C., and Mace, Lee M., "Operational Procedures for Estimating Wind Vectors From Geostationary Satellite Data," NOAA Technical Memorandum NESS 39, National Environmental Satellite Service, National Oceanographic and Atmospheric Administration, U.S. Department of Commerce, Washington, D.C., July 1972, 19 pp.

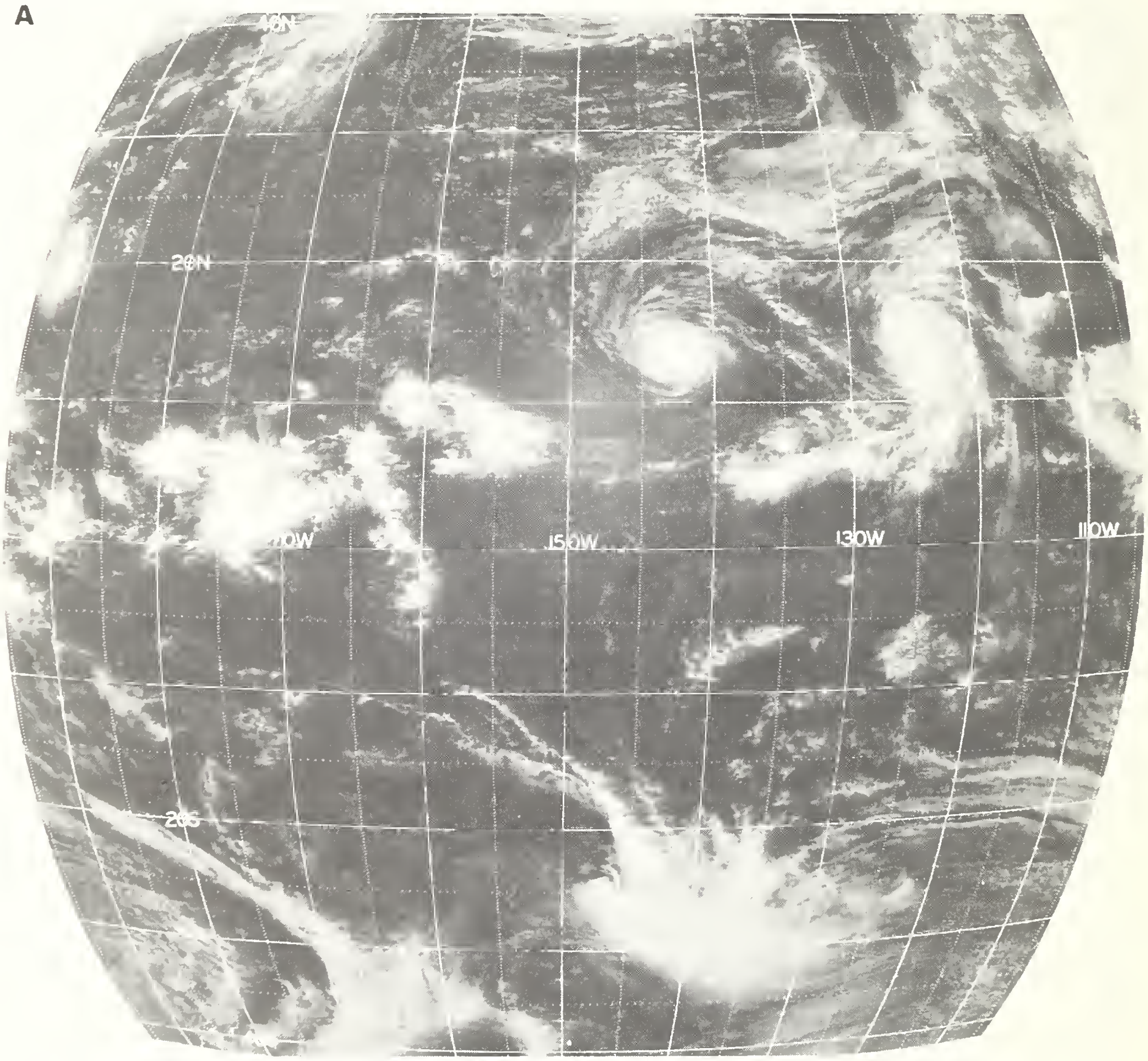

Figure 1.--(A) ATS-1 picture with a superposed geodetic grid (near 2200 GMT on Aug. 12, 1972; (B) objective streamline (solid lines) and isotach (broken lines) analyses for about 00 GMT on Aug. 13, 1972 (shaded areas indicate speeds of 20 kt and greater); and (C) vectors and relative vorticity. The shortest wind shafts represent computer vectors; the medium size shafts, manual vectors (for about 2200 GMT on Aug. 12, 1972; and the longest wind shafts, 850-mb rawin observations (for 00 GMT on Aug. 13, 1972. The vorticity isopleths are in units of 10^{-5} s^{-1} (zero isopleth omitted). The positive values represent counterclockwise circulation in both hemispheres; the cross hatching, anticyclonic vorticity; and shaded areas, cyclonic vorticity.

B

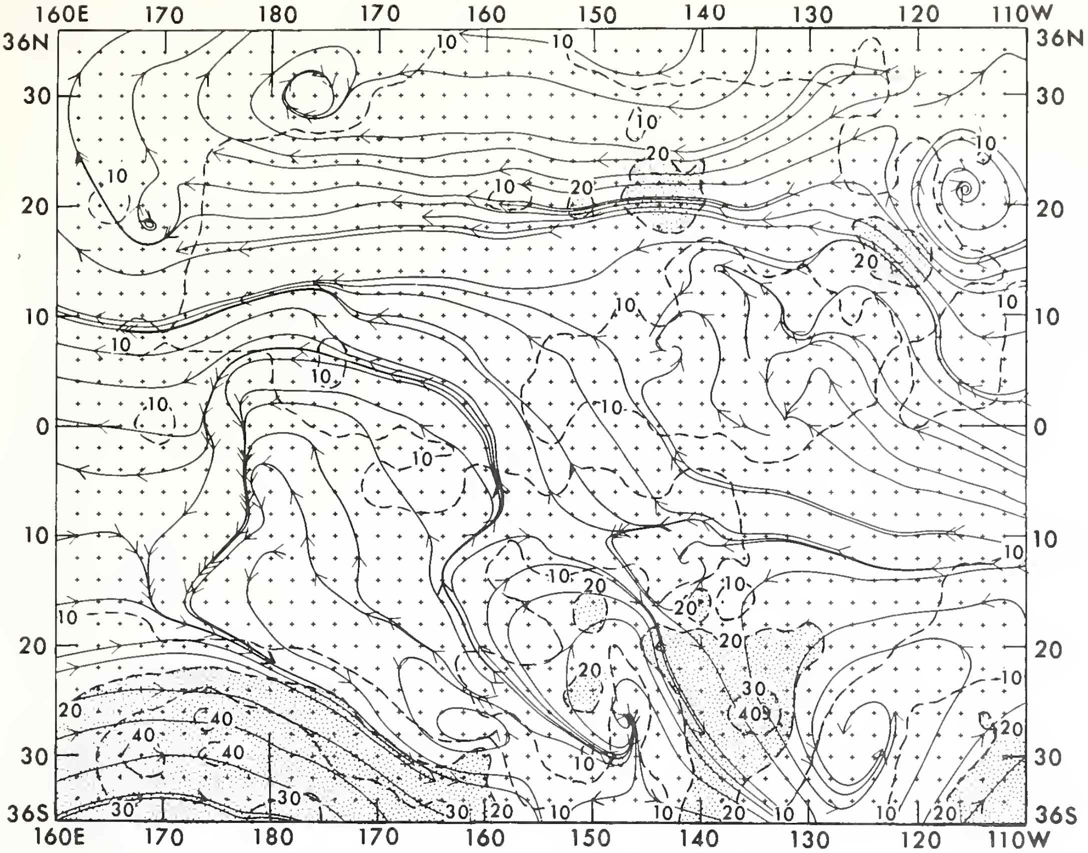
160E
170
180
170
160
150
140
130
120
110W
36N
30
20
10
0
10
20
30
36S
10
20
30
40
30
20
10

C

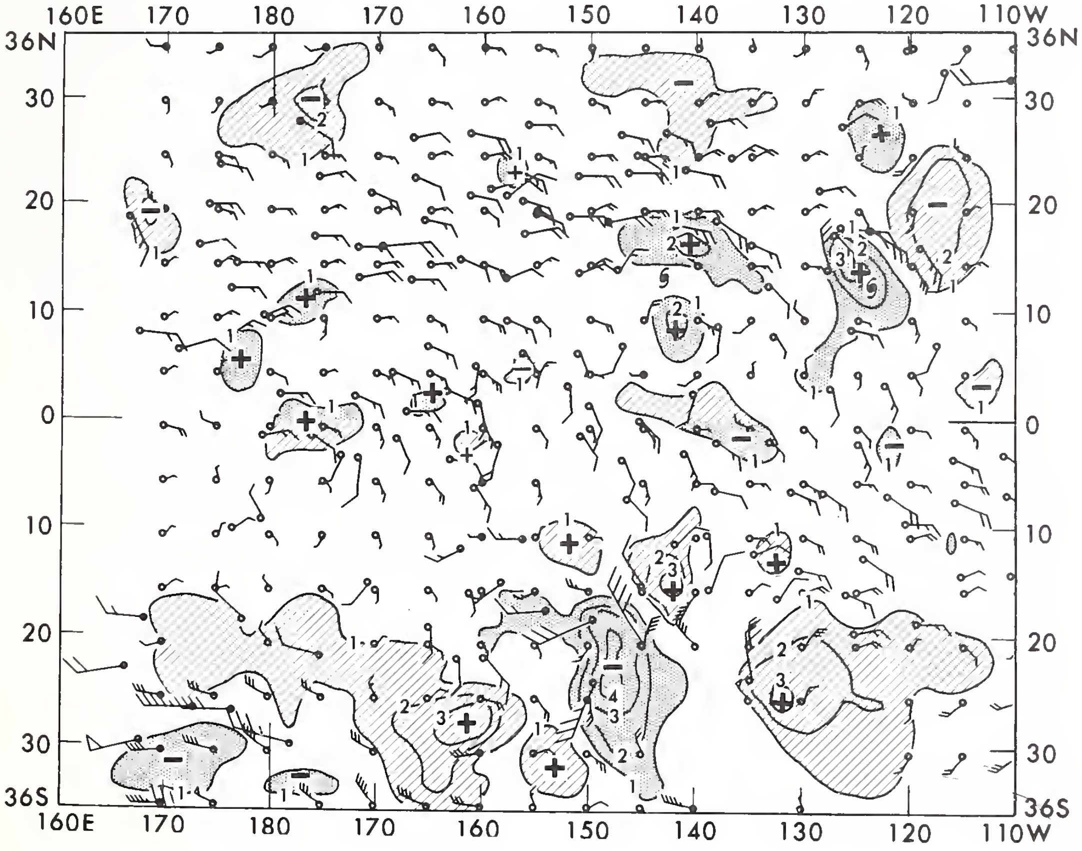
160E
170
180
170
160
150
140
130
120
110W
36N
30
20
10
0
10
20
30
36S
+
−
1
2
3
4

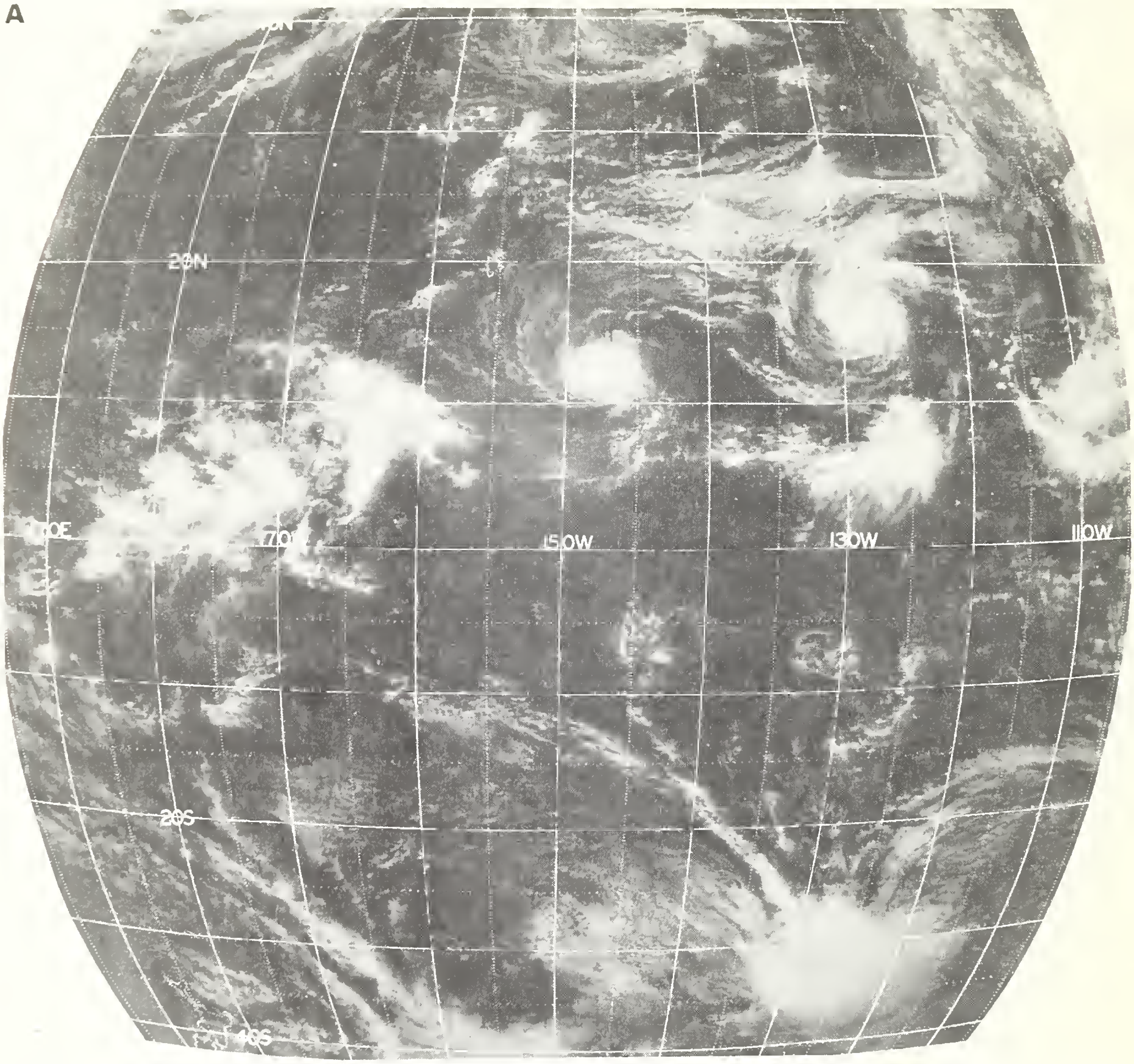

Figure 2.--Same as figure 1, but here (A) is near 2200 GMT on Aug. 13, 1972; (B), about 00 GMT on Aug. 14, 1972; and (C), about 00 GMT on Aug. 14, 1972.

B

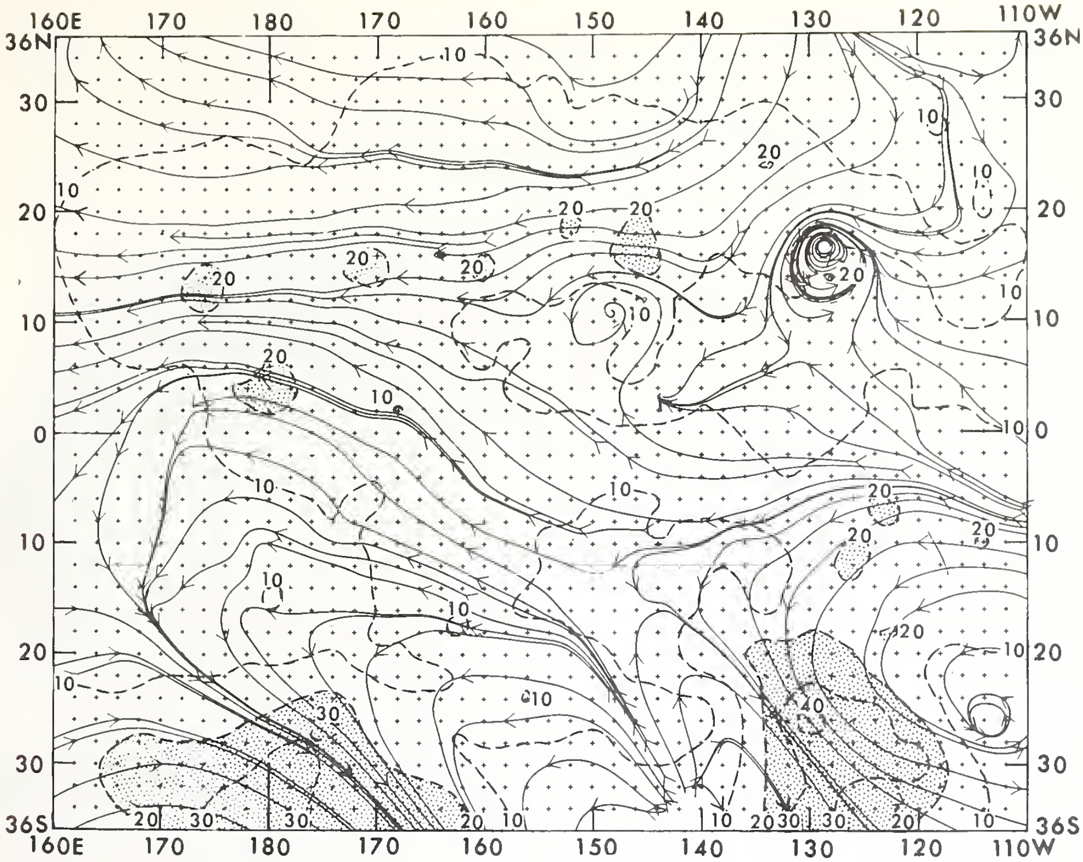
160E
170
180
170
160
150
140
130
120
110W
36N
30
20
10
0
10
20
30
36S
10
20
30
40

C

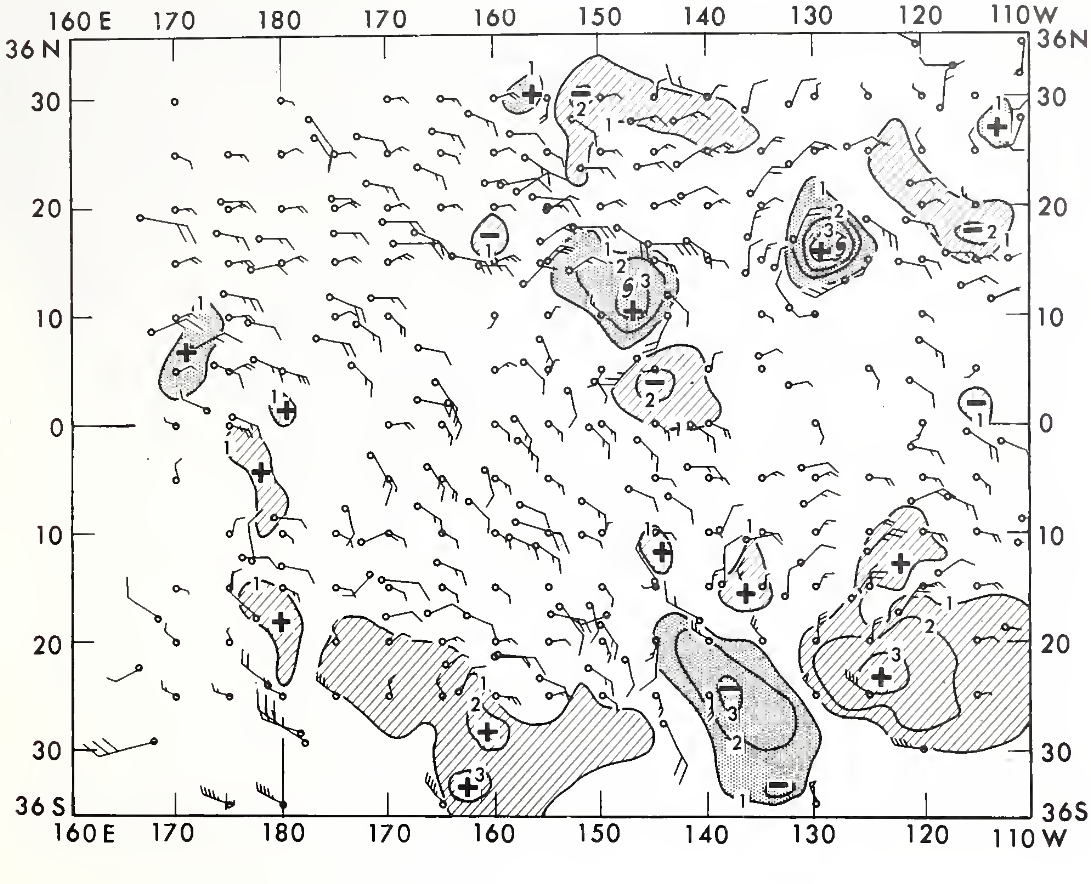
160 E
170
180
170
160
150
140
130
120
110 W
36 N
30
20
10
0
10
20
30
36 S
+
−
1
2
3

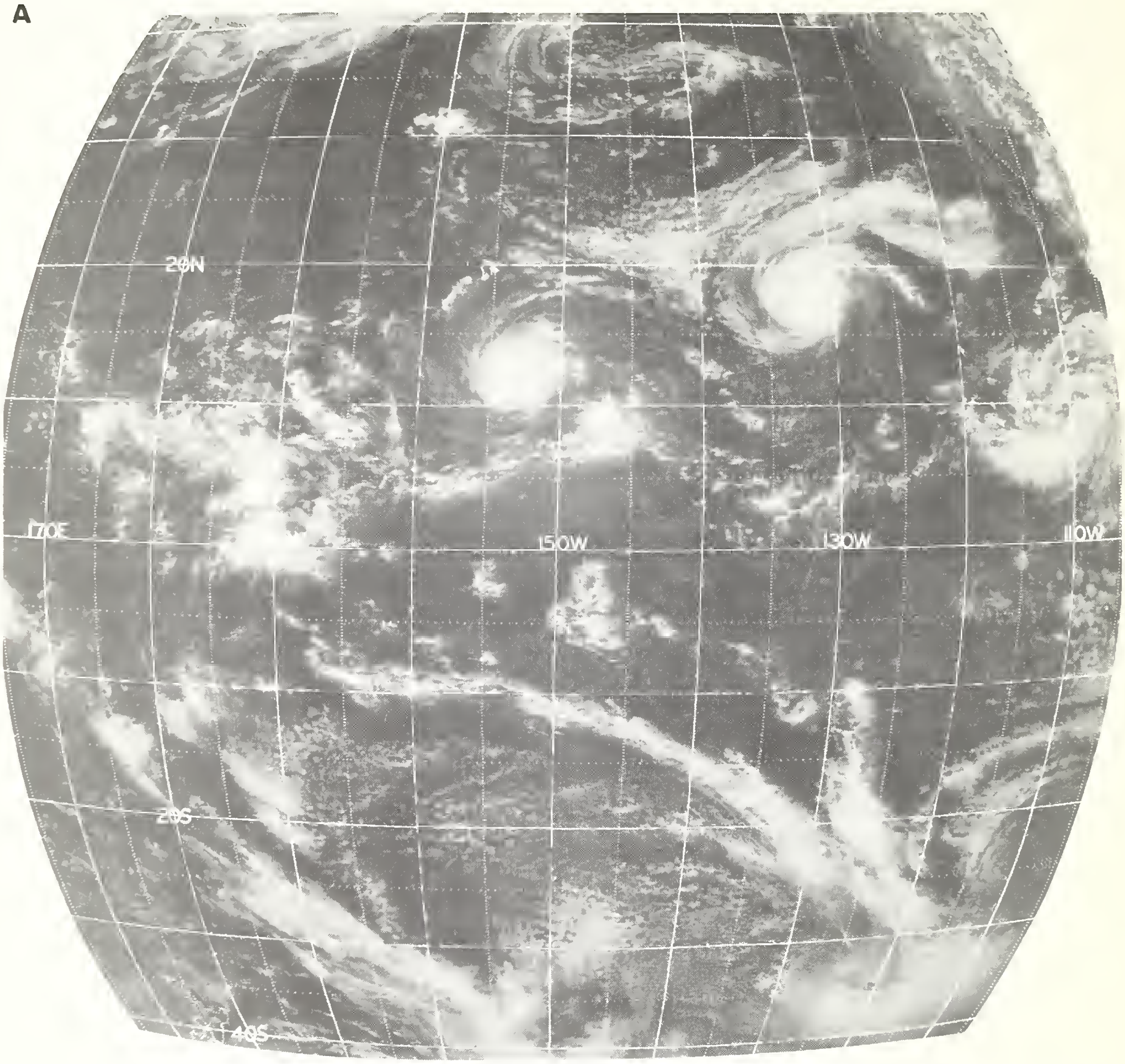

Figure 3.--Same as figure 1, but here (A) is near 2200 GMT on Aug. 14, 1972; (B), about 00 GMT on Aug. 15, 1972; and (C), about 00 GMT on Aug. 15, 1972.

B

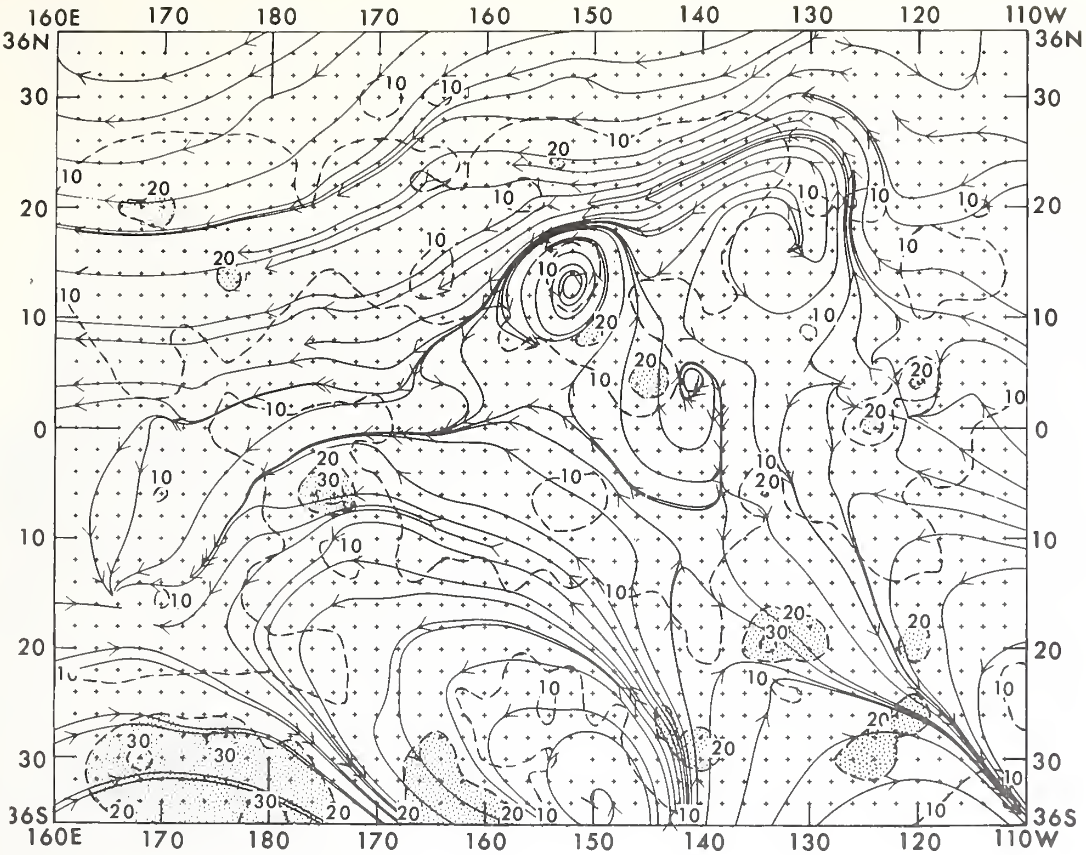
160E
170
180
170
160
150
140
130
120
110W
36N
30
20
10
0
10
20
30
36S
10
20
30

C

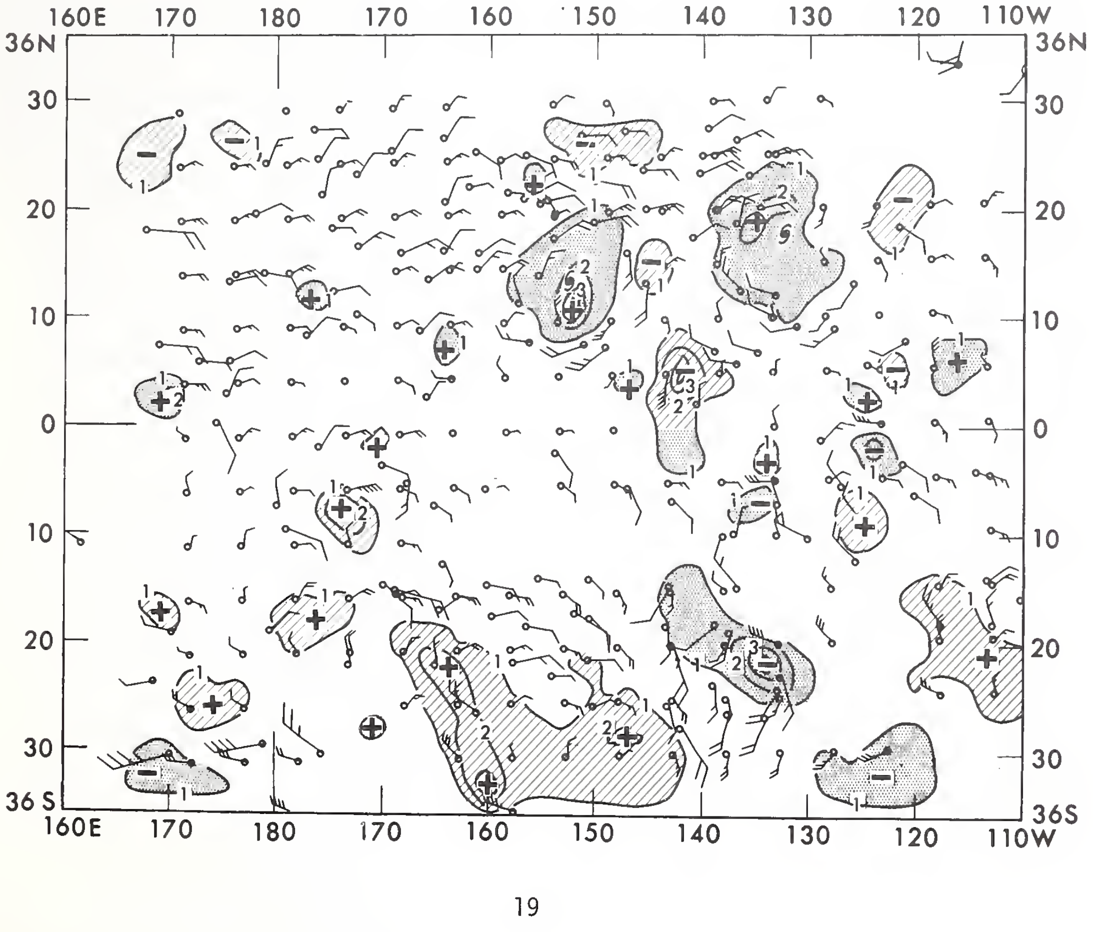
160E
170
180
170
160
150
140
130
120
110W
36N
30
20
10
0
10
20
30
36 S
36S
1
2
3

A

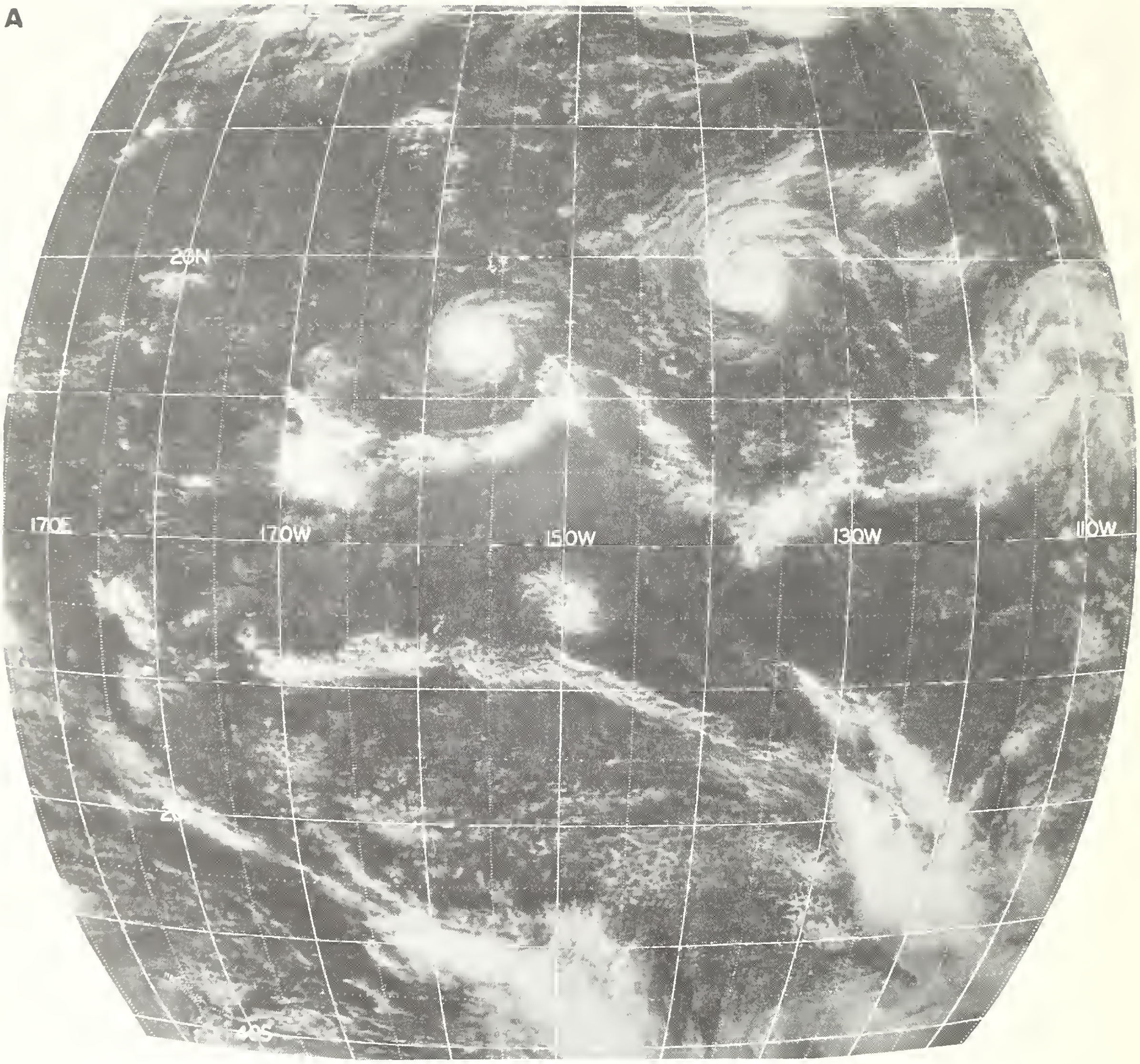

Figure 4.--Same as figure 1, but here (A) is 2200 GMT on Aug. 15, 1972; (B), about 00 GMT on Aug. 16, 1972; and (C), about 00 GMT on Aug. 16, 1972.

B

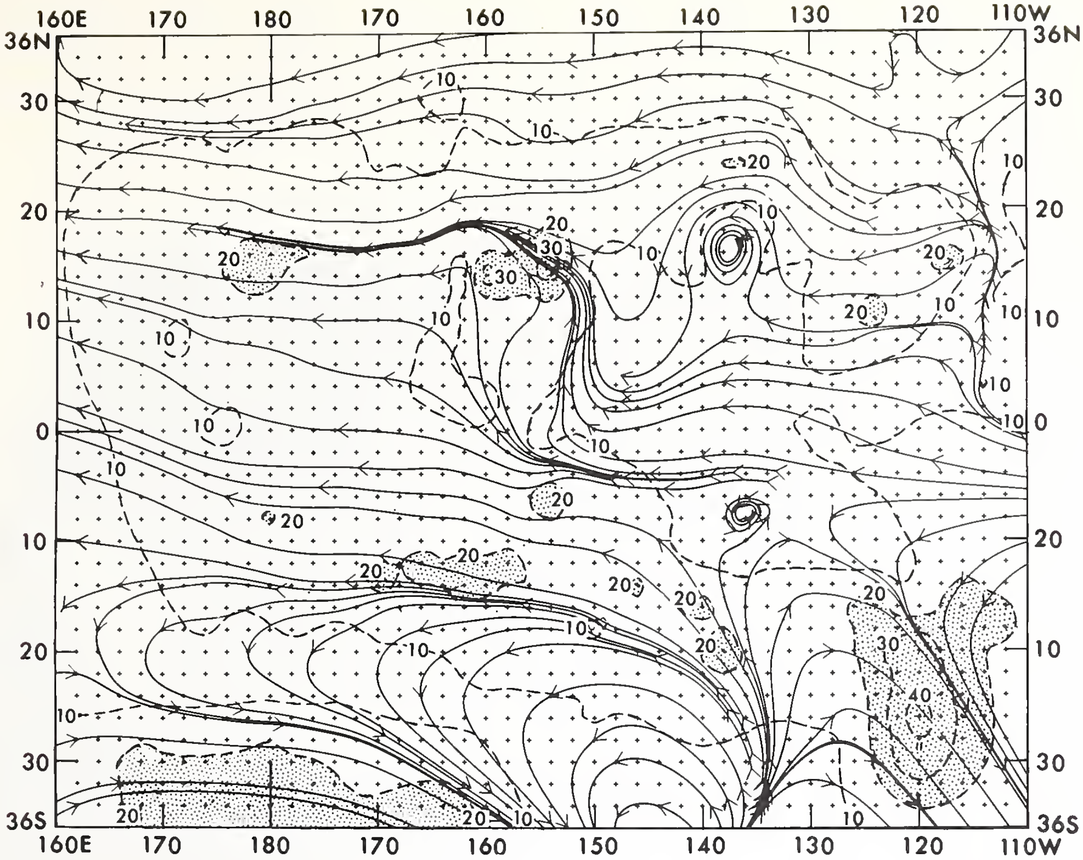
160E
170
180
170
160
150
140
130
120
110W
36N
30
20
10
0
10
20
30
36S
10
20
30
40

C

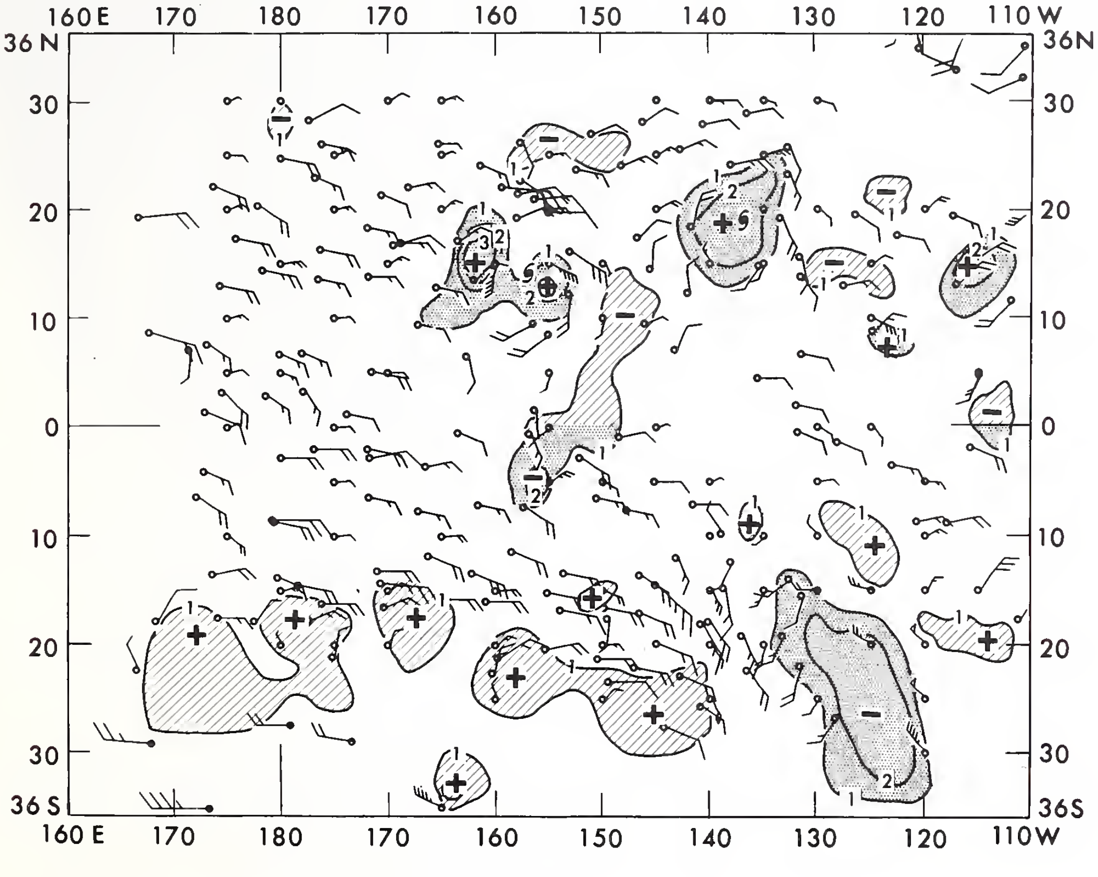
160 E
170
180
170
160
150
140
130
120
110 W
36 N
30
20
10
0
10
20
30
36 S
1
2
3
+
−

A

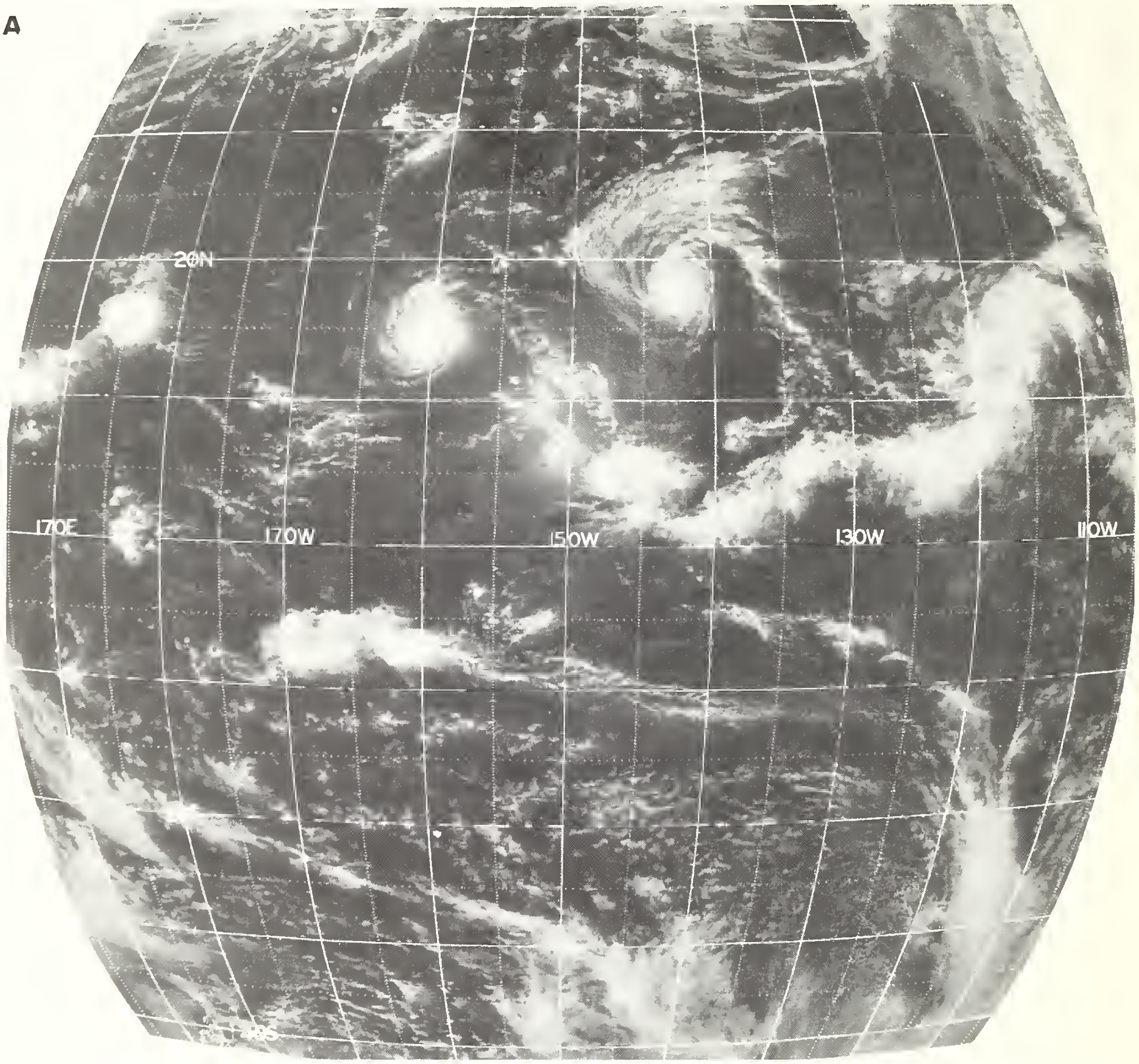

Figure 5.--Same as figure 1, but here (A) is near 2200 GMT on Aug. 16, 1972; (B), about 00 GMT on Aug. 17, 1972; and (C), about 00 GMT on Aug. 17, 1972.

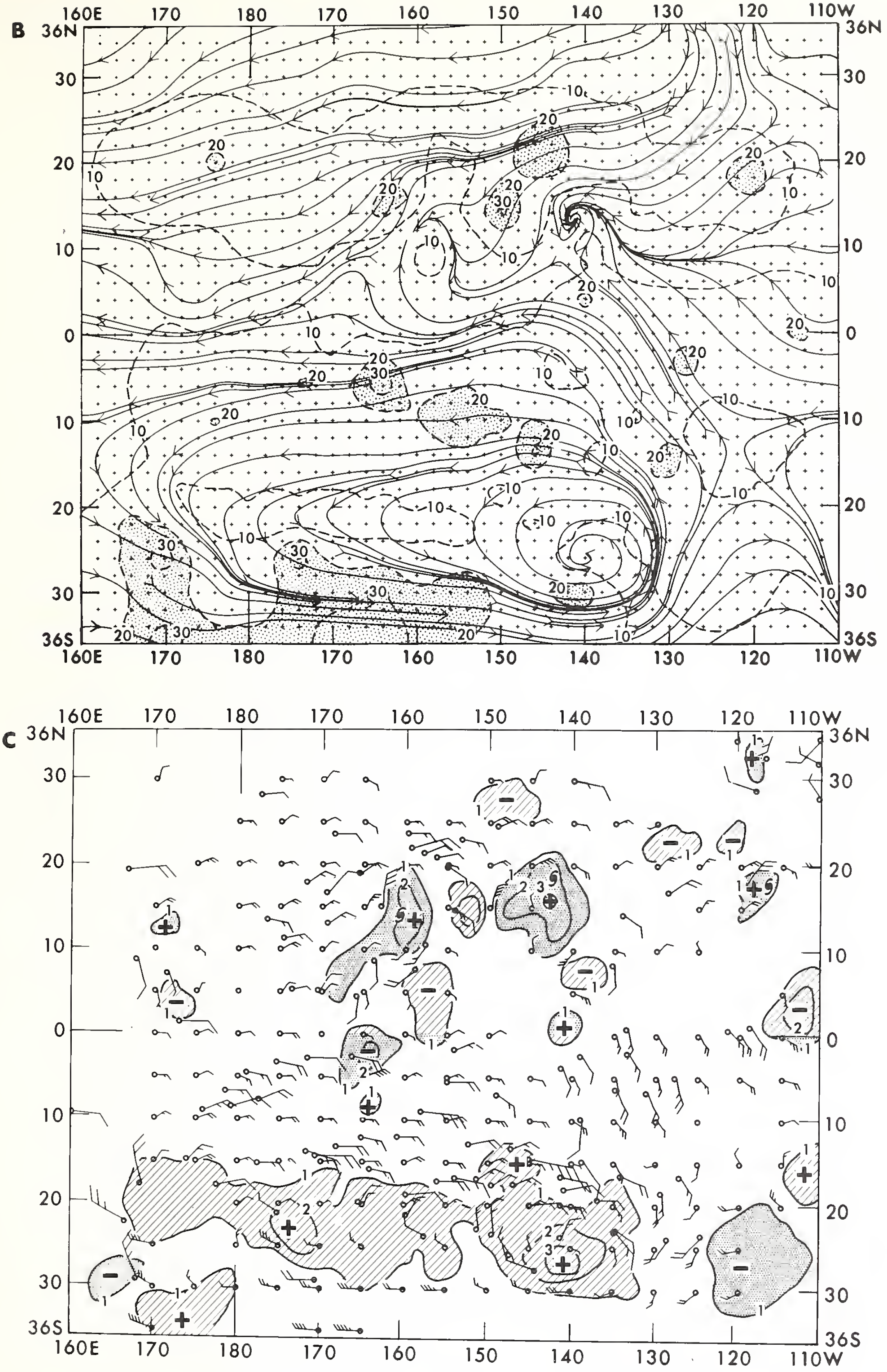
B
160E
170
180
170
160
150
140
130
120
110W
36N
30
20
10
0
10
20
30
36S
10
20
30
C
160E
170
180
170
160
150
140
130
120
110W
36N
30
20
10
0
10
20
30
36S
+
−
1
2
3

Table 1.--Means and root mean squares of magnitudes of vector deviations (kt) between each of three daily vector sets and their combined daily analysis for experiment 1

1972	Computer cloud vectors			Manual cloud vectors			00 GMT 850-mb rawinsonde vectors		
	$\overline{\|\Delta \mathbf{V}\|}$	rms	*N*	$\overline{\|\Delta \mathbf{V}\|}$	rms	*N*	$\overline{\|\Delta \mathbf{V}\|}$	rms	*N*
Aug. 13	3.6	4.8	183	3.1	3.9	104	5.5	7.0	23
14	3.1	3.8	160	2.9	3.4	125	4.3	5.2	25
15	3.9	4.9	157	3.4	4.0	105	4.7	5.6	22
16	3.6	5.0	81	2.8	3.6	128	3.5	4.2	23
17	2.8	3.6	153	3.0	3.6	64	3.0	3.8	28
Statistics of 5-day series	3.4	4.4	734	3.0	3.7	526	4.2	5.2	121
Statistics of 4-day series Aug. 14-17	3.3	4.3	551	3.0	3.7	422	3.8	4.7	98

$\overline{|\Delta \mathbf{V}|}$, mean of magnitude of vector deviations

rms, root mean square of $|\Delta \mathbf{V}|$

N, number of vectors

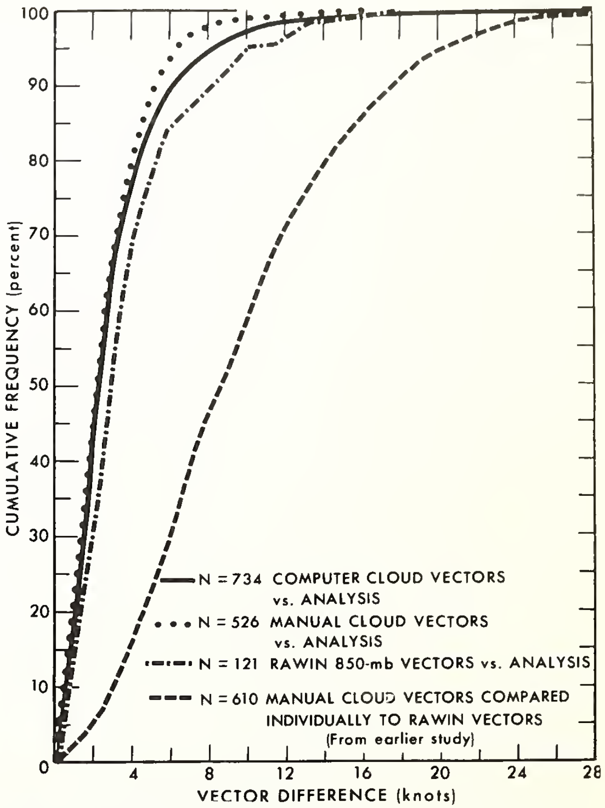

Figure 6.--Cumulative frequency of vector-magnitude deviations between wind data and the best analysis and cumulative frequency of vector-magnitude deviations between individual rawins and individual cloud vectors

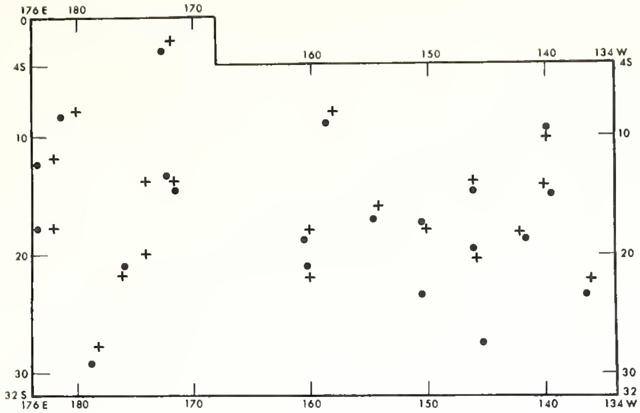

Figure 7.--Analysis area for experiment 2, a subarea of experiment 1, and locations of 20 grid points (crosses) and 21 rawin stations (dots) at which deviation statistics were derived for tables 2 and 3

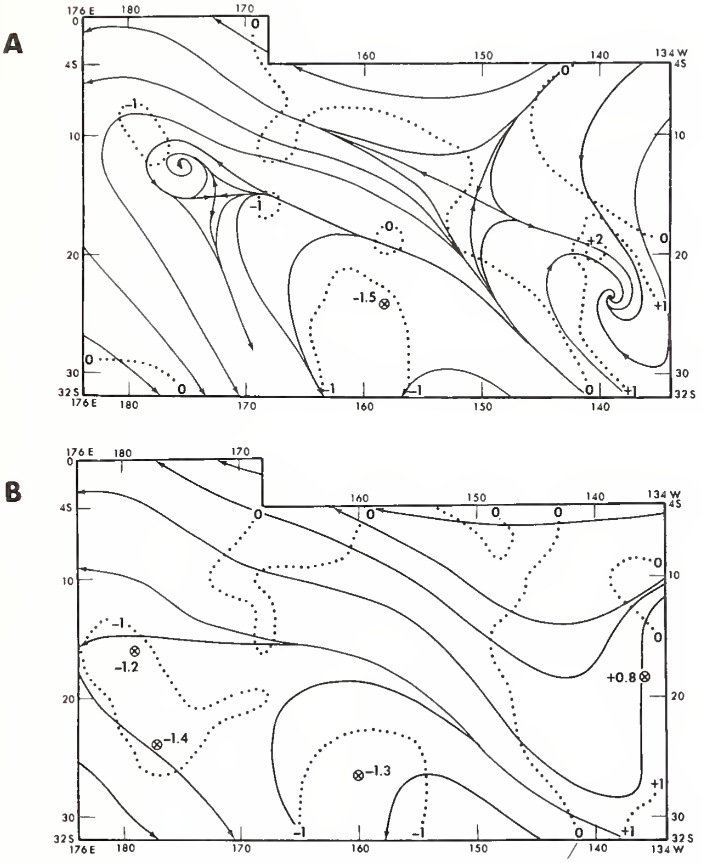

Figure 8.--(A) streamline analysis (solid lines) and relative vorticity isopleths (dotted lines) in units of 10^{-5} s^{-1} from 850 mb rawin-only data for 00 GMT on Aug. 14, 1972. (B) is the same as (A), but here the information is for selected manual vectors only.

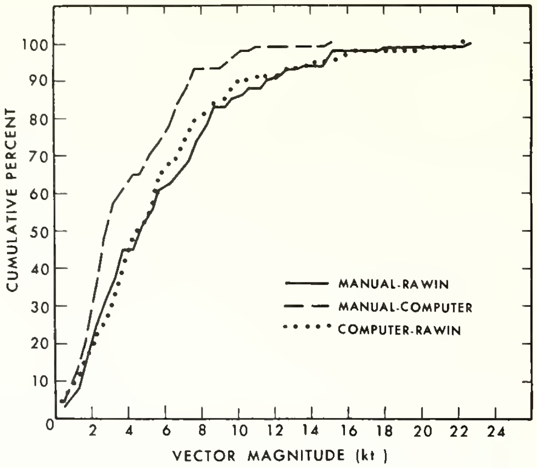

Figure 9.--Cumulative frequencies of vector-magnitude deviations between analyses at 20 grid points

Table 2.--Statistical summaries of the magnitudes of vector deviations (kt) between data and analyses for experiment 2 (4-day series)

Type of data	Rawins			Low-cloud vectors					
				Manual			Computer		
	$\overline{\vert\Delta \mathbf{V}\vert}$	rms	σ	$\overline{\vert\Delta \mathbf{V}\vert}$	rms	σ	$\overline{\vert\Delta \mathbf{V}\vert}$	rms	σ
Analysis of									
Rawin only	[3.4	3.9	1.8]*	7.8	9.0	4.4	7.6	8.7	4.3
Manual only	8.4	9.6	4.4	[2.7	3.0	1.4]*	6.7	8.2	3.9
Computer only	8.0	9.4	5.0	6.7	8.0	3.8	[2.7	3.0	1.3]*

*See text for the significance of the brackets.

$\overline{|\Delta \mathbf{V}|}$, mean of magnitude of vector deviations

rms, root mean square of $|\Delta \mathbf{V}|$

σ, standard deviation of $|\Delta \mathbf{V}|$

Table 3.--Statistical summaries of the magnitudes of vector deviations (kt) between analyses at 20 grid points near the data

Difference between:	Manual-rawin				Computer-rawin				Manual-computer			
Date (00 GMT)	$\overline{\vert\Delta \mathbf{V}\vert}$*	rms	$\overline{\Delta u}$	$\overline{\Delta v}$	$\overline{\vert\Delta \mathbf{V}\vert}$*	rms	$\overline{\Delta u}$	$\overline{\Delta v}$	$\overline{\vert\Delta \mathbf{V}\vert}$*	rms	$\overline{\Delta u}$	$\overline{\Delta v}$
Aug. 14, 1972	6.9	7.9	-3.7	2.6	6.6	7.4	-4.1	0.1	3.3	3.6	0.4	2.7
15	7.1	8.0	4.5	-0.7	5.9	6.7	-2.7	0.2	7.2	7.4	6.9	-0.4
16	5.5	7.7	-3.7	0.1	6.0	8.4	-0.9	0.9	4.3	5.6	-2.8	1.0
17	4.7	6.1	±0	-2.3	5.3	6.7	0.4	-2.2	2.0	2.4	0.2	-0.1
Combined 4 days	6.1	7.5	-0.7	-0.1	6.0	7.3	-2.0	0.5	4.2	5.1	1.2	0.8

*First columns, $(\Delta \mathbf{V})$ are means of individual vector magnitudes. For that reason, $\overline{|\Delta \mathbf{V}|} > (\overline{\Delta u}^2 + \overline{\Delta v}^2)^{1/2}$.

(Continued from inside front cover)

NESC 51 Application of Meteorological Satellite Data in Analysis and Forecasting. Ralph K. Anderson, Jerome P. Ashman, Fred Bittner, Golden R. Farr, Edward W. Ferguson, Vincent J. Oliver, and Arthur H. Smith, September 1969 (AD-697-033). Supplement (AD-740-017).

NESC 52 Data Reduction Processes for Spinning Flat-Plate Satellite-Borne Radiometers. Torrence H. MacDonald, July 1970. (COM-71-00132)

NESC 53 Archiving and Climatological Applications of Meteorological Satellite Data. John A. Leese, Arthur L. Booth, and Frederick A. Godshall, July 1970. (COM-71-00076)

NESC 54 Estimating Cloud Amount and Height From Satellite Infrared Radiation Data. P. Krishna Rao, July 1970. (PB-194-685)

NESC 56 Time-Longitude Sections of Tropical Cloudiness (December 1966-November 1967). J. M. Wallace, July 1970. (COM-71-00131)

NOAA Technical Reports

NESS 55 The Use of Satellite-Observed Cloud Patterns in Northern Hemisphere 500-mb Numerical Analysis. Roland E. Nagle and Christopher M. Hayden, April 1971. (COM-73-50262)

NESS 57 Table of Scattering Function of Infrared Radiation for Water Clouds. Giichi Yamamoto, Masayuki Tanaka, and Shoji Asano, April 1971. (COM-71-50312)

NESS 58 The Airborne ITPR Brassboard Experiment. W. L. Smith, D. T. Hilleary, E. C. Baldwin, W. Jacob, H. Jacobowitz, G. Nelson, S. Soules, and D. Q. Wark, March 1972. (COM-72-10557)

NESS 59 Temperature Sounding From Satellites. S. Fritz, D. Q. Wark, H. E. Fleming, W. L. Smith, H. Jacobowitz, D. T. Hilleary, and J. C. Alishouse, July 1972. (COM-72-50963)

NESS 60 Satellite Measurements of Aerosol Backscattered Radiation From the Nimbus F Earth Radiation Experiment. H. Jacobowitz, W. L. Smith, and A. J. Drummond, August 1972. (COM-72-51031)

NESS 61 The Measurement of Atmospheric Transmittance From Sun and Sky With an Infrared Vertical Sounder. W. L. Smith and H. B. Howell, September 1972. (COM-73-50020)

NESS 62 Proposed Calibration Target for the Visible Channel of a Satellite Radiometer. K. L. Coulson and H. Jacobowitz, October 1972. (COM-73-10143)

NESS 63 Verification of Operational SIRS B Temperature Retrievals. Harold J. Brodrick and Christopher M. Hayden, December 1972. (COM-73-50279)

NESS 64 Radiometric Techniques for Observing the Atmosphere From Aircraft. William L. Smith and Warren J. Jacob. January 1973. (COM-73-50376)

NESS 65 Satellite Infrared Soundings From NOAA Spacecraft. L. M. McMillin, D. Q. Wark, J.M. Siomkajlo, P. G. Abel, A. Werbowetzki, L. A. Lauritson, J. A. Pritchard, D. S. Crosby, H. M. Woolf, R. C. Luebbe, M. P. Weinreb, H. E. Fleming, F. E. Bittner, and C. M. Hayden, September 1973. (COM-73-50936/6AS)

NESS 66 Effects of Aerosols on the Determination of the Temperature of the Earth's Surface From Radiance Measurements at 11.2 μm. H. Jacobowitz and K. L. Coulson, September 1973. (COM-74-50013)

NESS 67 Vertical Resolution of Temperature Profiles for High Resolution Infrared Radiation Sounder (HIRS). Y. M. Chen, H. M. Woolf, and W. L. Smith, January 1974. (COM-74-50230)

NESS 68 Dependence of Antenna Temperature on the Polarization of Emitted Radiation for a Scanning Microwave Radiometer. Norman C. Grody, January 1974. (COM-74-50341/AS)

NESS 69 An Evaluation of May 1971 Satellite-Derived Sea Surface Temperatures for the Southern Hemisphere. P. Krishna Rao, April 1974. (COM-74-50643/AS)

PENN STATE UNIVERSITY LIBRARIES
A000072018408

AMERICAN REVOLUTION BICENTENNIAL
1776-1976